

Supplementary Material

Electroplating of Ni-W coating on Zn surface for durable Zn ion batteries

Khanothai Choonha-Anothai¹, Chengwu Yang², Meijing Wang³, Zhiqiang Dai³, Napat Kiatwisarnkij^{1,2}, Kittima Lolupiman^{2,4}, Xinyu Zhang³, Panyawat Wangyao¹, Jiaqian Qin²

¹Metallurgical Engineering Department, Faculty of Engineering, Chulalongkorn University, Bangkok 10330, Thailand.

²Center of Excellence on Advanced Materials for Energy Storage, Department of Materials Science, Faculty of Science, Chulalongkorn University, Bangkok 10330, Thailand.

³State Key Laboratory of Metastable Materials Science and Technology, Yanshan University, Qinhuangdao 066004, Hebei, China.

⁴Nanoscience and Technology Interdisciplinary Program, Chulalongkorn University, Bangkok 10330, Thailand.

Correspondence to: Dr. Panyawat Wangyao, Metallurgical Engineering Department, Faculty of Engineering, Chulalongkorn University, Phayathai Road, Bangkok 10330, Thailand. E-mail: panyawat.w@chula.ac.th

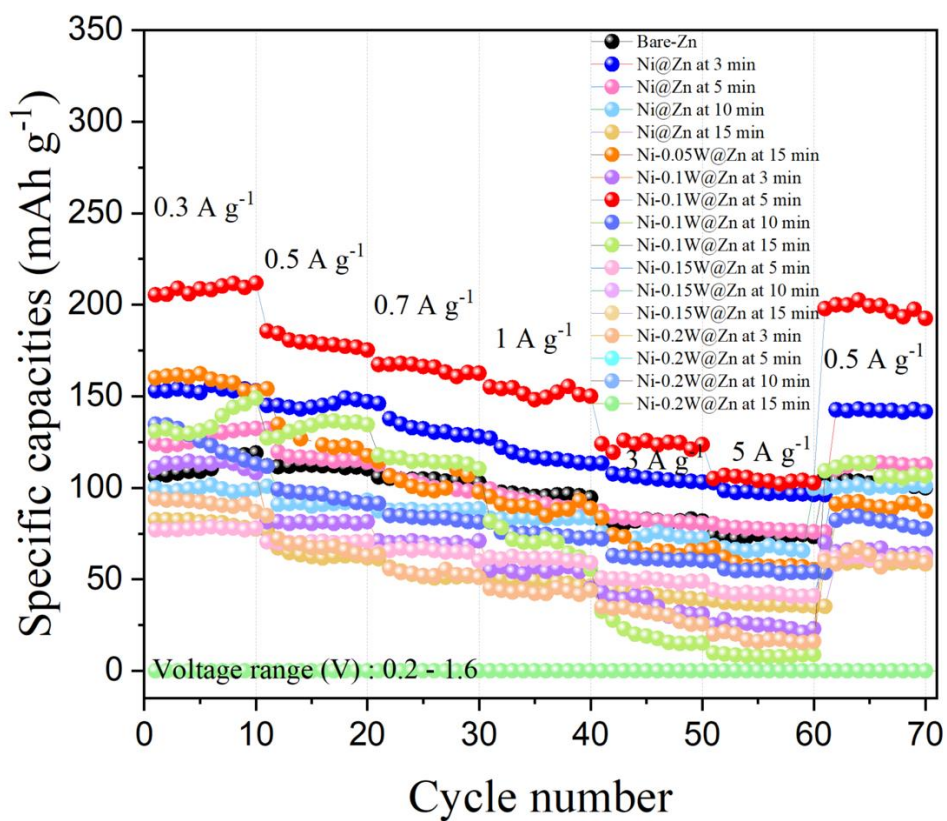


Figure S1. Rate performance in Bare-Zn, Ni@Zn, and Ni-W@Zn with different concentrations and deposition times.

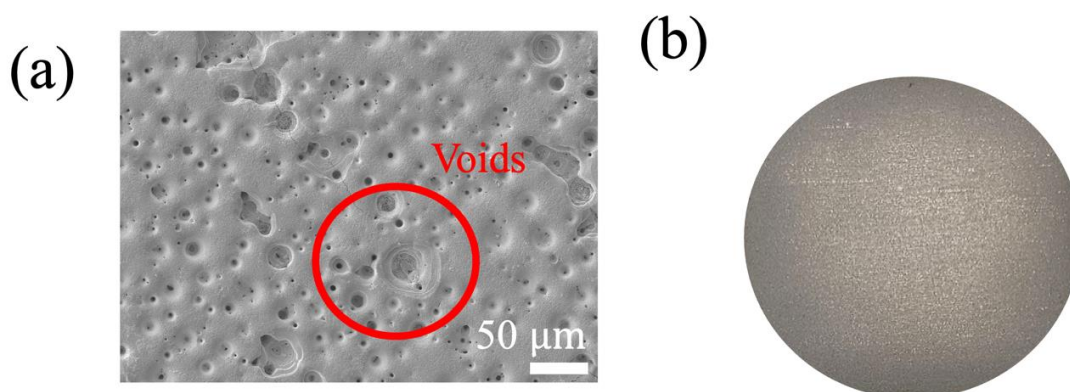


Figure S2. The SEM image (a) and optical image (b) of Ni-W electroplating on Zn foil at Tungsten concentration of 0.1M for 180 s.

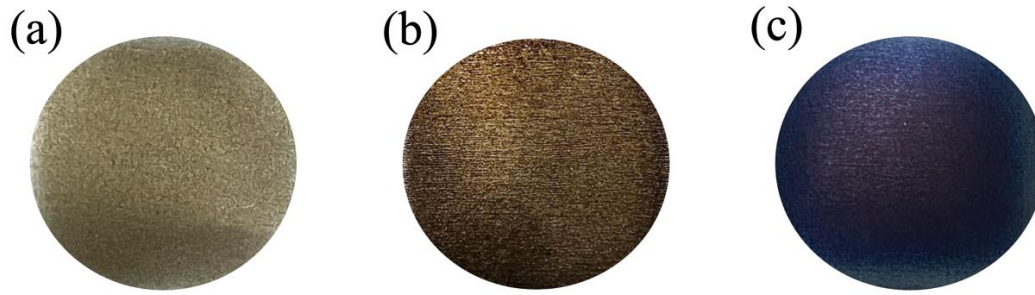


Figure S3. The optical images of Ni-W electroplating on Zn foil at Tungsten concentration of than 0.15 M for (a) 600 s, (b) 900 s and (c) Ni-W electroplating on Zn foil at Tungsten concentration of 0.2 M for 300 s.

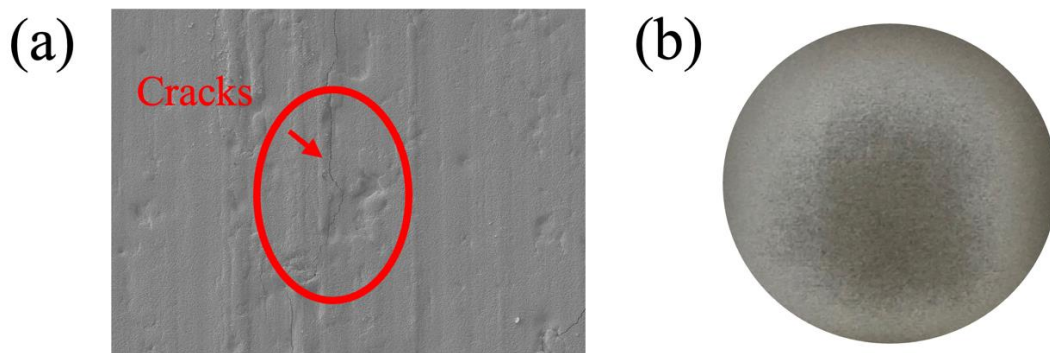
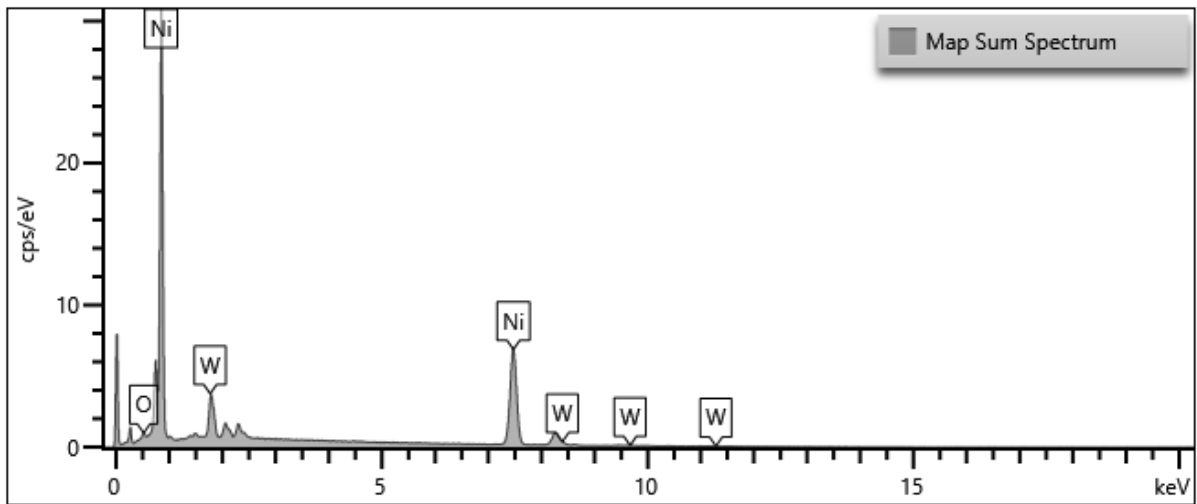


Figure S4. The SEM image (a) and optical image (b) of Ni-W electroplating on Zn foil at Tungsten concentration of 0.15M for 300 s.



Map Sum Spectrum					
Element	Signal Type	Line	Wt%	Wt% Sigma	Atomic %
O	EDS	K series	0.56	0.05	2.19
Ni	EDS	K series	86.94	0.21	93.51
W	EDS	M series	12.51	0.21	4.30
Total			100.00		100.00

Figure S5. The element content of Ni and (0.1 M) W on Zn foil at a deposition time of 300 s. (Initial state of the sample)

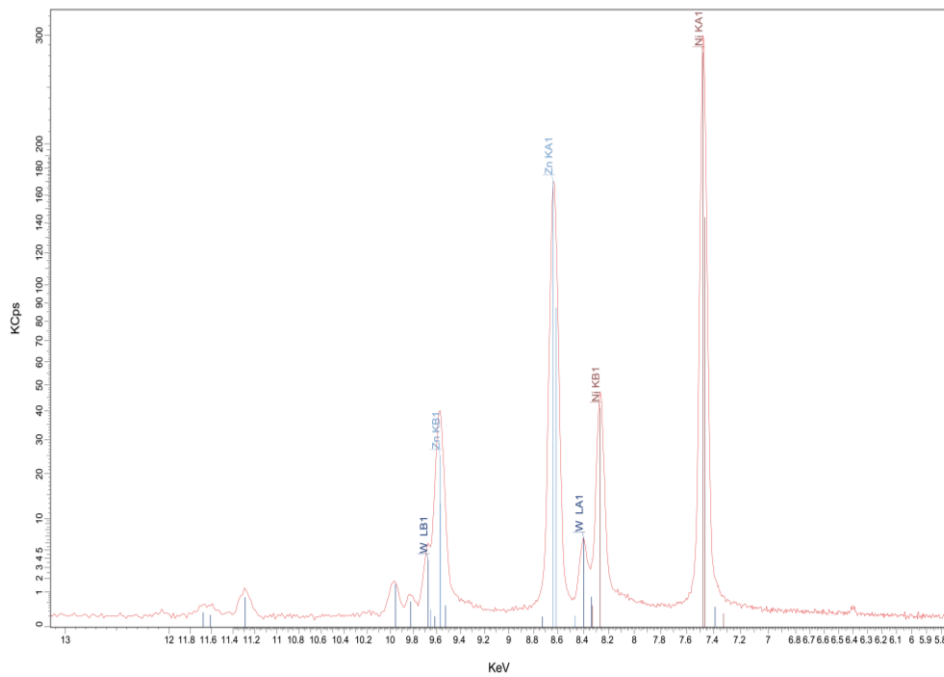


Figure S6. Results of X-ray fluorescence (XRF) analyses, with spectra in the range of 0-8 KeV illustrated for Ni-0.1W@Zn.

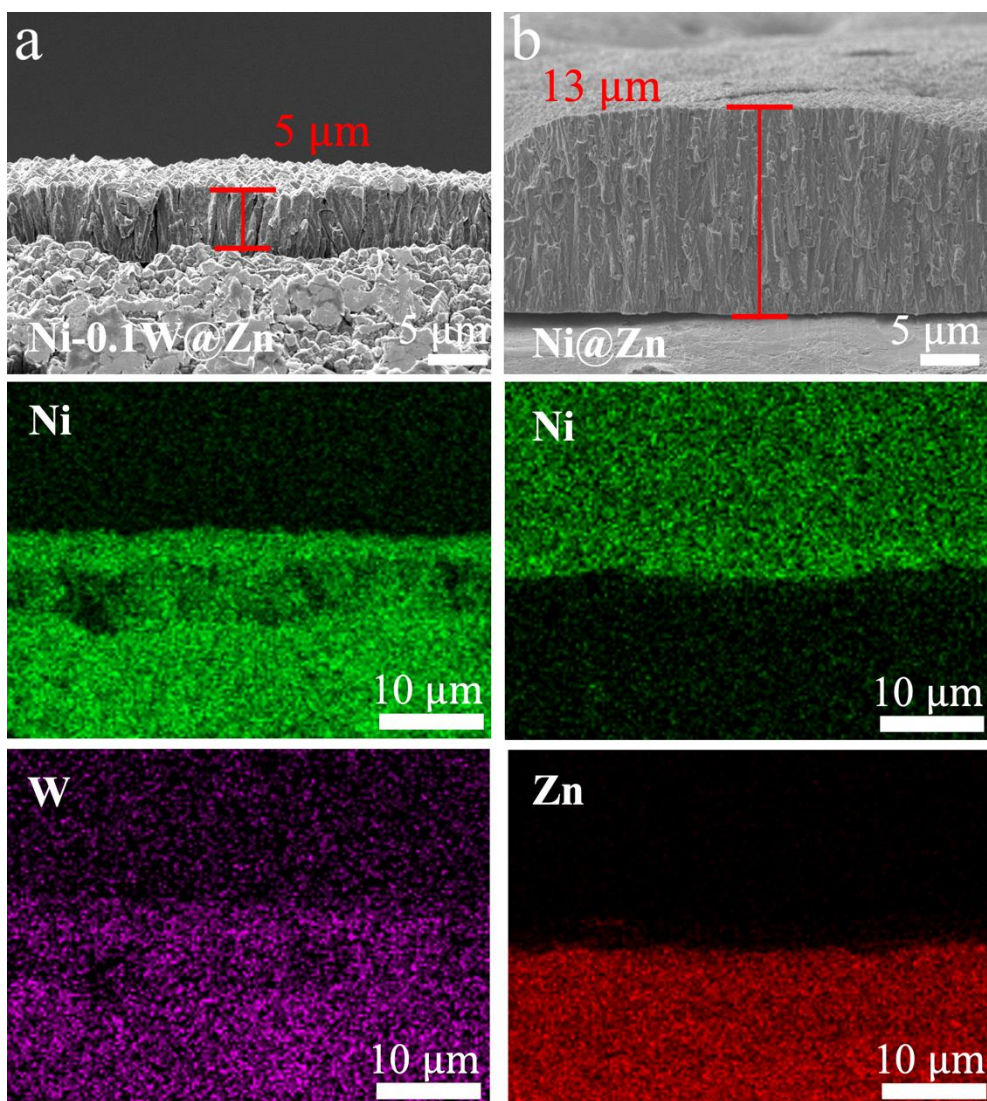


Figure S7. Element mapping images of (a) Ni-0.1W@Zn and (b) Ni@Zn

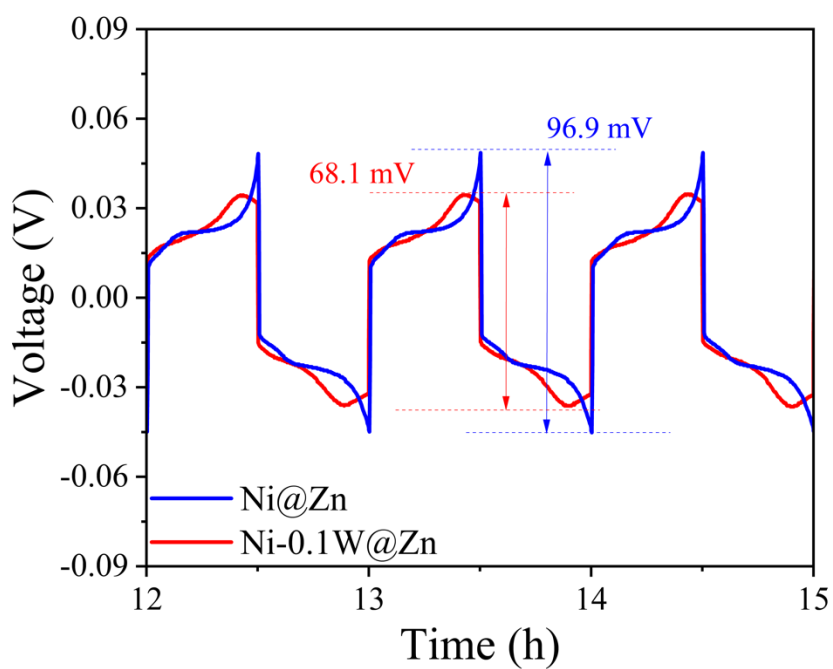


Figure S8. The initial overpotential of symmetric cells in Ni@Zn and Ni-0.1W@Zn at 1 mA cm⁻²

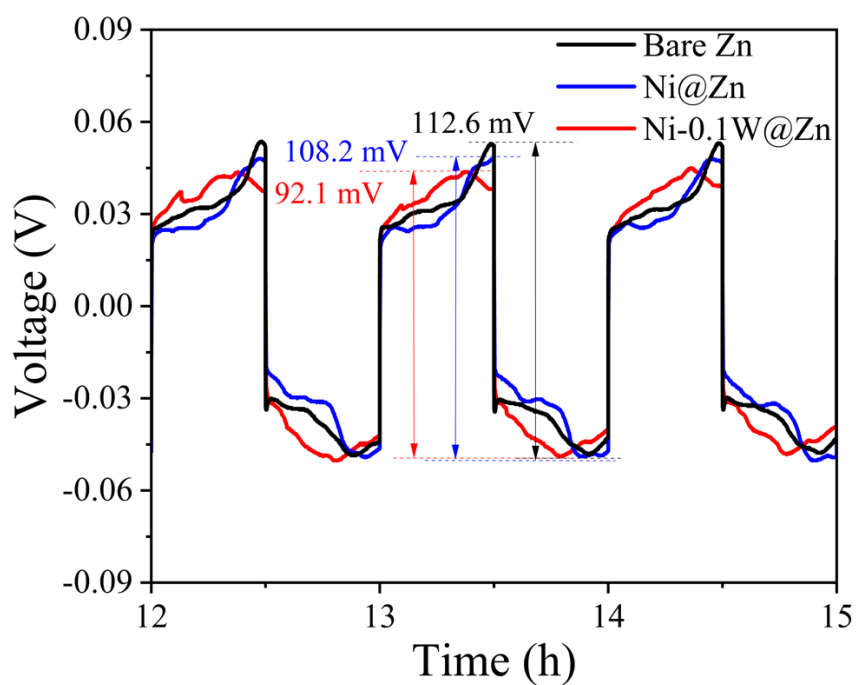


Figure S9. The initial overpotential of symmetric cells in bare-Zn, Ni@Zn and Ni-0.1W@Zn at 2 mA cm⁻²

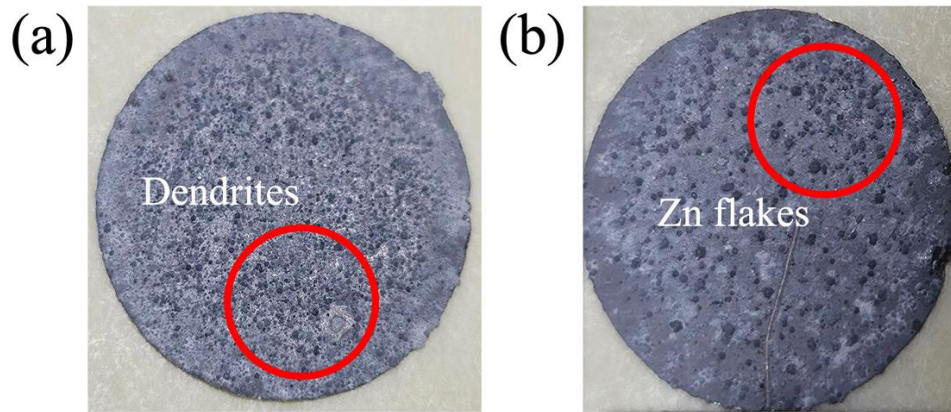


Figure S10. Optical images of anode side after symmetric cells tests; (a) Bare-Zn and (b) Ni@Zn

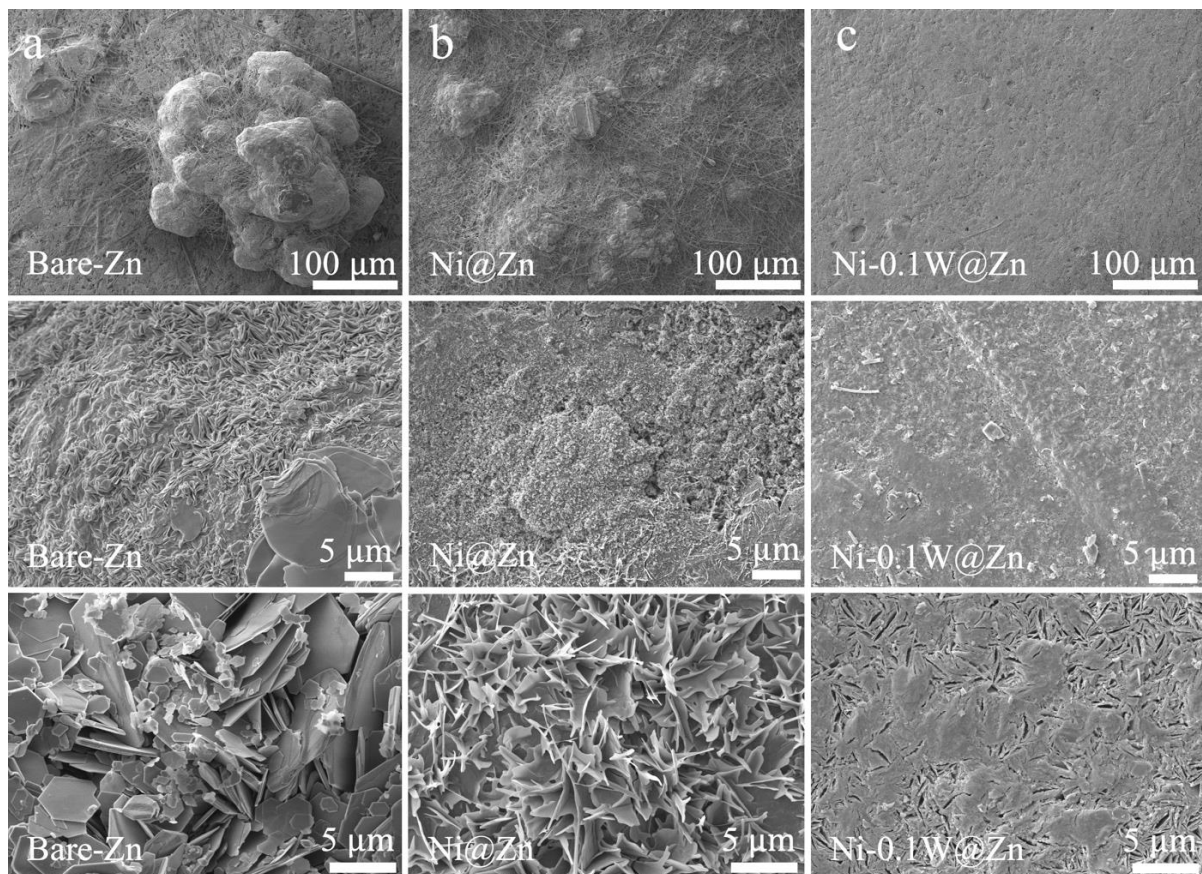


Figure S11. SEM images of (a) Bare-Zn after 100 h at 1 mA cm^{-2} and (b) Ni@Zn after 150 h at 1 mA cm^{-2} and (c) Ni-0.1W@Zn after 1300 h at 2 mA cm^{-2} .

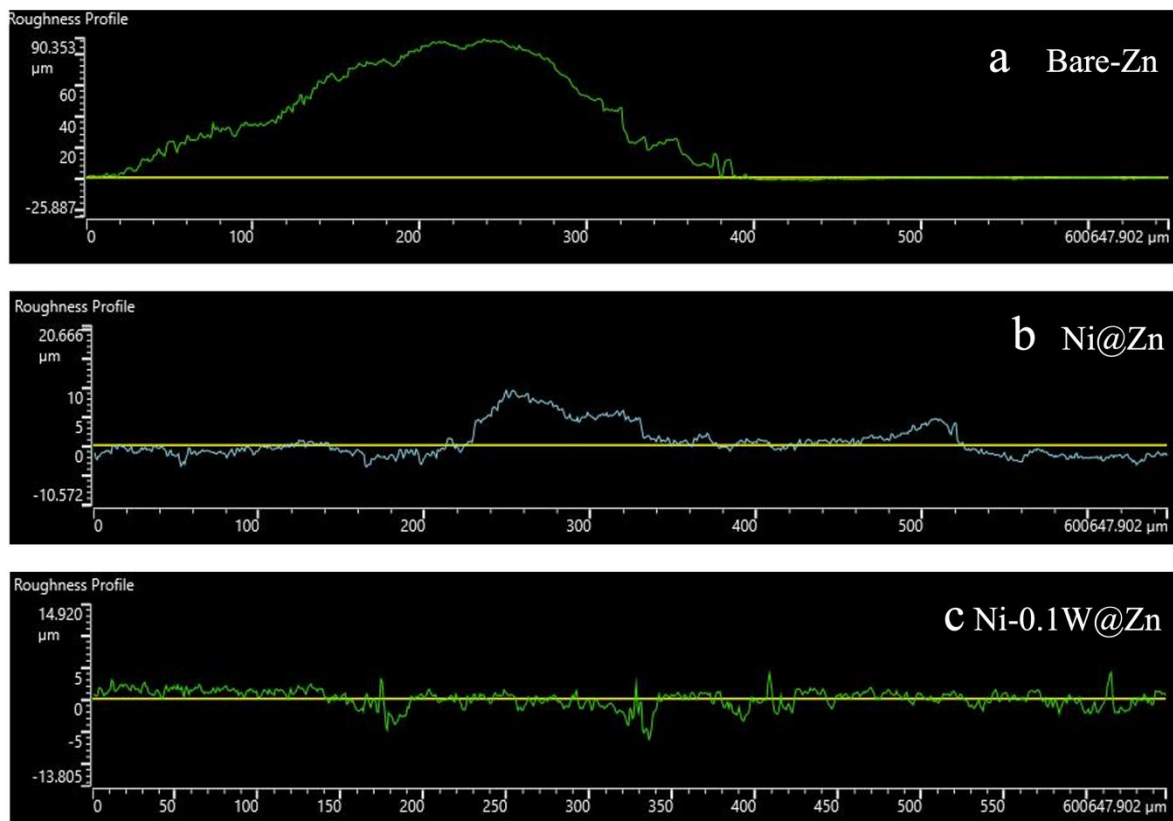


Figure S12. Surface roughness curves of (a) Bare-Zn and (b) Ni@Zn and (c) Ni-0.1W@Zn

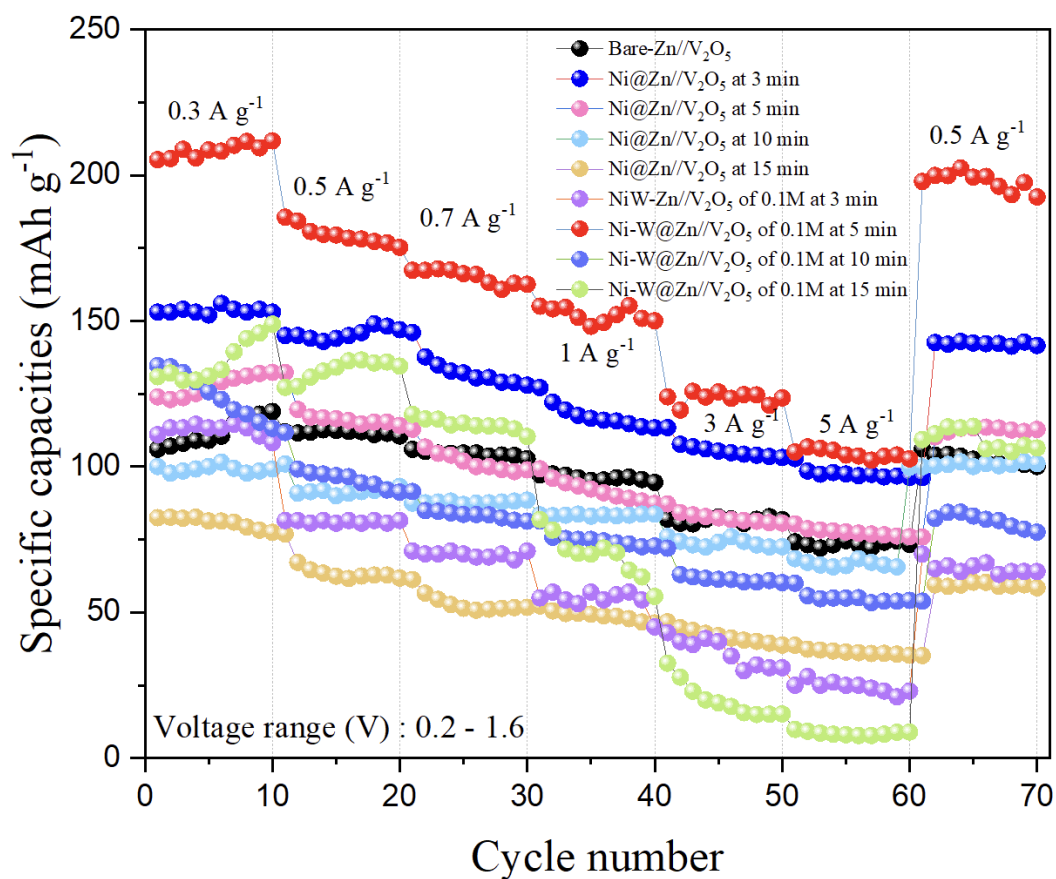


Figure S13. Rate performance in Bare-Zn, Ni@Zn and Ni-W@Zn with a different current density.

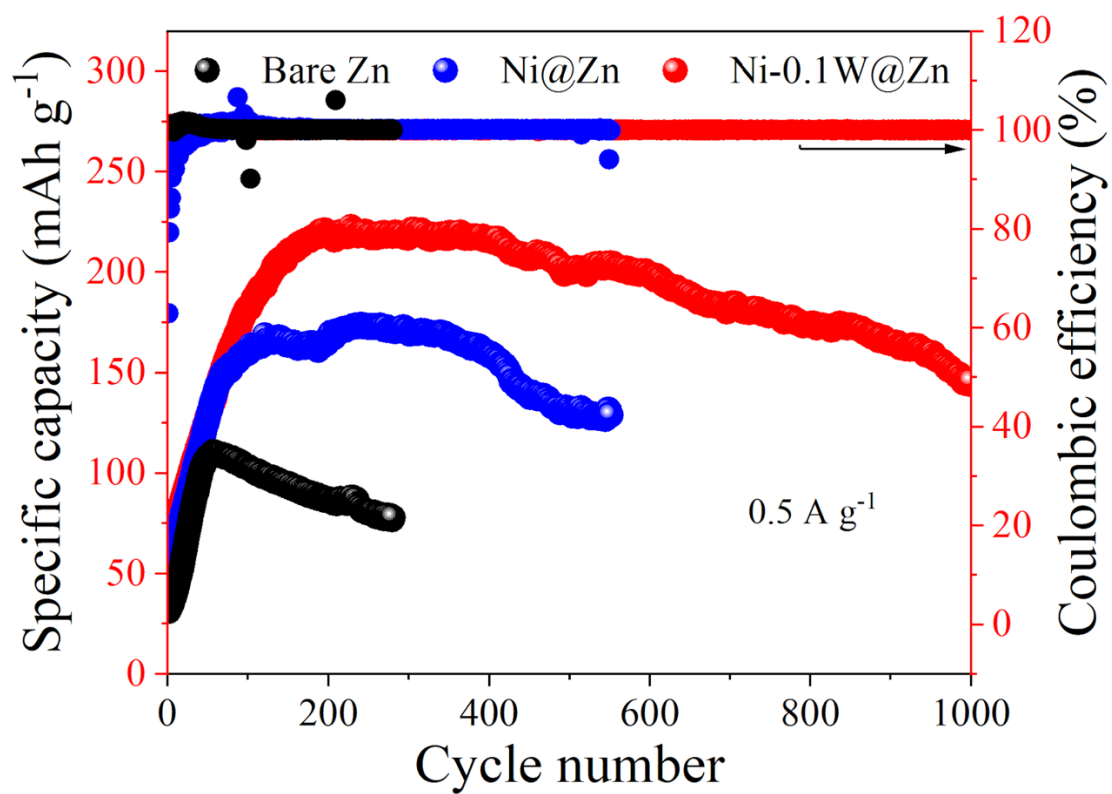


Figure S14. Cycling stabilities of bare-Zn/ V_2O_5 , Ni@Zn/ V_2O_5 and Ni-0.1W@Zn/ V_2O_5 at 0.5 mA cm^{-2} .

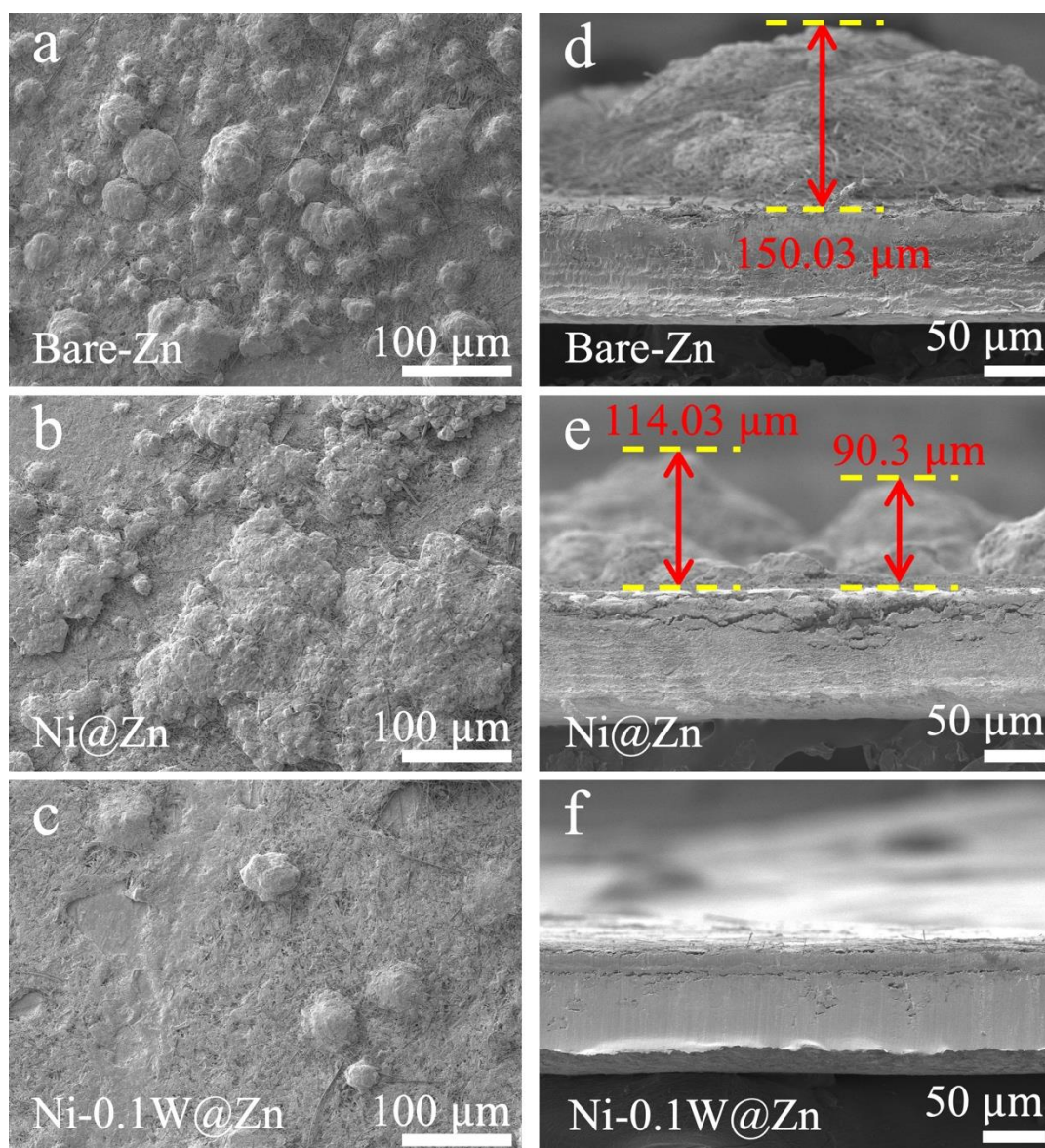


Figure S15. SEM images of (a) Bare-Zn, (b) Ni@Zn and (c) Ni-0.1W@Zn and cross-section of (d) Bare-Zn, (e) Ni@Zn and (f) Ni-0.1W@Zn after cycling stability tests at 1 A g⁻¹